CLM-R221

UKAEA

Report

THE PHYSICS OF MAGNETIC CONFINEMENT CONFIGURATIONS: TOKAMAK THEORY AND EXPERIMENT

D. C. ROBINSON

CULHAM LABORATORY
Abingdon Oxfordshire
1982

C/18

Available from H. M. Stationery Office

£3.00

THE PHYSICS OF MAGNETIC CONFINEMENT CONFIGURATIONS: TOKAMAK THEORY AND EXPERIMENT

D C Robinson
Culham Laboratory, Abingdon, Oxon, OX14 3DB, UK
(Euratom/UKAEA Fusion Association)

ABSTRACT

The basic tokamak configuration consists of a strong toroidal magnetic field together with a weak poloidal field generated by a toroidally directed plasma current which is induced by transformer action. The joule dissipation associated with this current heats the plasma to temperatures of about 1 keV. Auxiliary heating by means of neutral beams has been used to raise the ion temperature to about 6-7 keV; high frequency wave heating has raised the temperature to about 2 keV and appears to be very promising. The strength of the plasma current is limited by magnetohydrodynamic stability considerations. If the current is too high, a disruptive instability appears which can terminate the plasma current and damage the walls of the containing vessel. The magneto hydrodynamic stability of the tokamak has been demonstrated experimentally for values of beta (ratio of mean plasma pressure to magnetic pressure) up to 3%, however theoretical predictions indicate higher values of beta are possible. For future large reactor-like tokamaks, values of beta of between 5 and 10% are required. Ion energy confinement is observed to be close to that predicted theoretically. The electron energy confinement however is anomalous, but its scaling is such that a moderate size tokamak should ignite. High values of the Lawson product, i.e. density x energy confinement time, have been achieved in small high field tokamaks and in medium size low field tokamaks. Present values are within a factor of 10 of those required for ignition and are adequate for systems which produce sufficient thermonuclear power to compensate for the additional heating power. An important plasma physics problem is the control of impurities associated with wall interactions. A variety of divertor experiments are now in operation and these have demonstrated some control of impurities. The remaining physics problems appear to be an improvement in the value of beta, some control of disruptions, the practical viability of a continuously operating tokamak and the burn of deuterium-tritium fuel. Key theoretical problems are seen as a convincing theory of the anomalous electron transport, an understanding of the disruptive instability, impurity transport, and methods of current drive.

The next generation of large tokamaks such as JET, TFTR, JT-60, T-15 should produce parameters close to those required to demonstrate the scientific feasibility of fusion in the tokamak system. Significant amounts of fusion power, in the region of 10's of MW, may be produced by the late 1980's. A number of conceptual tokamak reactor designs now exist which indicate that fusion might be an alternative to the fast breeder fission reactor as they are both characterised by high capital cost, low fuel costs, and extensive fuel reserves.

Invited lecture for the Latin-American Workshop on Plasma Physics and Controlled Nuclear Fusion Research, Cambuquira, Minas Gerais, Brazil, 8-12 February 1982.

January 1982
cms

ISBN 0 85311 109 X

1 INTRODUCTION

The tokamak* story begins in the mid 1950's when it was recognised that the addition of a toroidal magnetic field to a toroidal pinch would improve the stability of the discharge against the most dangerous forms of instability. The combination of the self magnetic field of the plasma current and the externally produced toroidal field leads to helical field lines and to the most important tokamak parameter, the safety factor "q". This is the number of times the field line encircles the major axis, in circling once around the minor axis. From the geometry of the field lines and for a circular cross section of the magnetic surfaces

$$q = \frac{rB_\phi}{RB_\theta} \qquad (1)$$

where r = minor radius, R = major radius of the magnetic surfaces, B_ϕ the toroidal field and B_θ the poloidal field. Fig.1 shows the co-ordinates and fields for a tokamak. The early theoretical work demonstrated two forms of stabilised pinches: first the tokamak in which stability against gross instabilities is achieved by geometric means i.e. by making $q > 1$ at all radii, and second the reverse field pinch in which $q < 1$ and stability is achieved by shear and a conducting wall close to the plasma. The tokamak system requires much larger externally applied toroidal fields, B_ϕ than do reverse field pinches where $B_\phi \sim B_\theta$. In the mid 1950's the United Kingdom and the United States of America concentrated on the apparently cheaper pinch while leaving the tokamak approach to the Soviet Union.

The early Soviet work was initiated by Yavlinski[1] and co-workers who in 1956 first studied the tokamak principle in a linear device and later in a toroidal device. For a number of years the work was bedevilled by problems associated with impurities and adequate means of diagnosing the plasma. The impurity problem was partly solved by progressing from insulating tori to vacuum vessels of stainless steel with baking and finally to tori with refractory metal limiters to reduce wall damage. On diagnostics the key problem was to diagnose the main plasma parameters, the electron and ion temperatures. However in the initial phases of this programme only the plasma energy content was measured by using a diamagnetic loop and the analysis was unconvincing at that time, but in fact it has now turned out that it was correct. The success of the devices was largely measured in terms of the electrical conductivity namely getting the loop voltage down to a few volts/turn.

Towards the end of the 1960's the main features of the tokamak design and performance as we know them today were established. The key features of the

*An acronym for toroidal magnetic chamber in Russian.

standard tokamak are shown in Fig.2 particularly the iron core, metal wall torus, tungsten or molybdenum limiter, copper stabilising shell, vertical field windings, and toroidal field coils. Particular features noted at the time included the disruptive instability when q at the limiter fell below about 3, the limited operating range for density bounded by runaway at low values and disruption at high values, the electron temperature from soft x-rays and diamagnetism several times the conductivity temperature and that the equilibrium was in good agreement with theory and the energy containment was substantially more than the Bohm confinement time.

Outside the Soviet Union the tokamak was considered somewhat difficult to understand because of the coupling between heating and containment and the difficulty with diagnosing the main plasma parameters. In 1969 Thomson scattering measurements were carried out on the tokamak T3 by a joint Culham/Kurchatov team which showed beyond question that all the claims for the performance of the tokamak were justified[2].

This success together with the rather poor performance of other systems at that time led to a rapid worldwide concentration on tokamaks. In the last 12 years the main effort on fusion has been on tokamaks and there has been a very substantial advance in parameters as well as in understanding. This advance is summarised in Table 1 where we compare the plasma parameters 1969 - 1981. For example the plasma current has risen from 130 kA on T3 to 2MA on DIII, the energy containment time has risen from 10 ms to 100 ms, the ion temperature has risen from 500 eV to 7keV while the peak electron temperature has risen from 1.5 keV to 3.5 keV.

TABLE 1

Tokamak Parameters

	1969	1981
I_p	130 kA	2000 kA
τ_E	10 ms	100 ms
T_i	500 eV	7500 eV
n_e	$5 \times 10^{13} cm^{-3}$	$10^{15} cm^{-3}$
T_e	1500 eV	3500 eV
τ_p	70 ms	12 s
q	> 3	> 1.4
$\beta(0)$	< 1%	12%

The advance in the tokamak parameters can be summarised in terms of the Lawson parameters $n\tau_E$ and T_i and these are shown in Fig.3.

2 BASIC CONFIGURATION AND GROSS STABILITY PROPERTIES

The basic tokamak configuration is illustrated in Fig.1. A strong toroidal magnetic field B_ϕ generated by an external toroidal solenoid is supplemented by a weak poloidal field B_θ which is generated by a toroidally directed plasma current induced by transformer action. The resultant helical magnetic field lines generate nested axisymmetric magnetic surfaces that confine the plasma particles. The strength of the plasma current is limited by MHD stability considerations and MHD stable tokamak operation is obtained typically for $q(0) \sim 1$ on axis and $q(a) \sim 3$ at the plasma edge. The expansion of the plasma ring with current flowing round it, is counter-balanced by adding a vertical magnetic field, B_z parallel to the major axis of the torus of appropriate sign and magnitude. This may be provided by external windings or using a highly conducting shell surrounding the plasma in which image currents are induced as the plasma moves in major radius. The usefulness of the shell is limited by the time constant for dissipation of the image currents.

In the absence of the conducting shell the inhomogeneity of the vertical magnetic field will lead to instability in the vertical direction unless $\frac{\partial B_z}{\partial R} < 0$. This requirement corresponds to an additional quadrupole field which produces a convex maintaining field. Instability also occurs in the horizontal direction unless $0 > \frac{R}{B_z}\frac{dB_z}{dR} > -3/2$ so that careful design of the vertical field windings is required or active feedback must be used. The presence of the quadrupole field reflects itself in the shape of the plasma column, in particular a plasma elongated in the vertical direction is produced if $\frac{\partial B_z}{\partial R} > 0$. The production of non-circular plasmas is of particular interest in optimising the plasma energy content or beta in a tokamak. Equilibrium in a minor cross section is made up of an inward force due to B_θ, an outward force due to the plasma pressure and any compression of the toroidal field, B_ϕ. This balance is represented by the Bennett[3] pinch relation

$$\beta_\theta I^2 = 2Nk(T_e + T_i) \qquad (2)$$

where N is the number of electrons per unit length, T_e and T_i are the mean electron and ion temperatures respectively. The outward shift of the plasma in a tokamak is related to the value of poloidal beta, β_θ. There is a limiting value of $\beta_\theta = R/a$ beyond which the equilibrium displacement of the plasma outwards is so large that the outer magnetic surfaces are no longer closed and a separatrix is formed. However, if the plasma is heated quickly so that magnetic flux is conserved then there is no such equilibrium limitation[4].

One of the chief difficulties with tokamaks is that their gross stability is sensitive to the distribution of the plasma current and plasma pressure, quantities which are difficult to control. As the toroidal field is very much larger than the poloidal field the helical displacement of the plasma as a whole is prevented if this wavelength exceeds the circumferential length of the plasma everywhere i.e. $q = L_\theta B_\phi / L_\phi B_\theta > 1$ where L_ϕ and L_θ are the circumferential lengths in the toroidal and poloidal directions respectively. However, higher mode deformations require larger values of q for stability. In addition the existence of a small amount of resistivity permits instabilities known as resistive tearing modes to appear. These can be stable for appropriate current distributions. Figure 4 shows how close the conducting wall has to be to the current carrying region of the plasma to give stability for a reverse field pinch when compared with the stable current distribution in a tokamak with no conducting wall. For the tokamak configuration the toroidal geometry also exerts a stabilising effect on instabilities driven by the plasma pressure making strong magnetic shear and a conducting shell unnecessary. The limiting beta in this system is probably set by instabilities driven by the plasma pressure growing in regions of unfavourable curvature known as ballooning modes. Figure 5 shows the deformation of a toroidal plasma subject to such instabilities. The optimum beta values obtained to date vary between 5 and 10% for a D-shaped cross section plasma. However resistive ballooning modes are unstable at much lower values of beta and may impose a lower limit to the value of beta.

3 CONFINEMENT IN THE TOKAMAK

Typical orbits of charged particles in the tokamak configuration are shown in Fig.6. As the ideal configuration is axisymmetric then the canonical angular momentum in the toroidal configuration is conserved from which it follows, Tamm (1961)[5], that all particle excursions across the poloidal flux surfaces are bounded by a gyro radius in the poloidal field, ρ_θ, that is $(mkT)^{\frac{1}{2}}/eB_\theta$. Thus it is the poloidal field component which is important for transport and for diffusion. The variation of the toroidal field across the magnetic surfaces leads to the formation of trapped particles as shown in Fig.6. As a result of these particles transport is enhanced, relative to the simple classical Pfirsch-Schluter[6] transport, for a highly collisionless or banana regime plasma. With the effective collision frequency, ν, lower than the bounce frequency of the trapped particles, the diffusion coefficient is proportional to $\nu\rho_\theta^2$. Most plasmas with ohmic heating alone are not in this collisionless regime but are in an intermediate regime, the so called plateau regime where the diffusion coefficient is independent of collison frequency. An interesting distinctive feature of transport in a tokamak is that the radial inward drift of the plasma is much larger than would be expected from a simple classical formula; the poloidal field controls the inward drift rather

than the toroidal field. A further interesting phenomena is the bootstrap effect in which in a collisionless plasma when beta poloidal is greater than $(R/a)^{\frac{1}{2}}$ it becomes possible to reach a steady state regime in which the external poloidal flux need not be supplied by a transformer but the discharge current is maintained by supplying plasma mass and heat inputs to maintain a radial outward flow.

The principal classical energy loss mechanism is ion heat conduction; the coefficients for electron heat conduction and particle transport are smaller by $(m_e/m_i)^{\frac{1}{2}}$. Classical predictions for the minimum tokamak reactor size required to reach ignition in a deuterium-tritium plasma are very favourable, the plasma minor radius would be less than 1 metre. As has been the case throughout controlled fusion research there are also anomalous transport mechanisms which proceed via co-operative effects. The observed electron heat conduction coefficients are very much enhanced relative to classical predictions and they are comparable with the ion heat conduction values. The particle diffusion coefficient behaves approximately like the electron heat conduction but of a smaller magnitude.

One view is that small scale micro-instabilities are responsible for the anomalous loss of energy. Particular instabilities which may be responsible are:-

toroidally induced drift universal instabilities,
dissipative trapped electron instabilities,
ion temperature gradient instabilities,
temperature gradient driven micro-tearing modes.

The physics of the saturation mechanism for the nonlinear evolution of these micro instabilities is far from clear.

4 TOKAMAK DEVICES

Figure 2 shows the standard arrangement for a traditional tokamak device. The poloidal flux has been conventionally provided by an iron core transformer with the plasma current forming a secondary of the transformer. Many devices now dispense with the iron core and the thick conducting shell. An air-core transformer permits a larger flux swing but requires more energy from the power supply, and it requires a small stray field inside the torus. The stabilising copper shell was originally considered necessary for two reasons; (i) it provides through eddy currents the necessary vertical magnetic field to give equilibrium to the toroidal plasma; (ii) it assists in stabilising helical instabilities by again providing appropriate eddy currents. A typical copper shell would have a time constant for control of the equilibrium of the order of 100 ms. For pulses of longer duration it is necessary to provide a vertical field with external windings. A stabilising shell has now been shown to be unnecessary and control of the equilibrium using

vertical field coils together with feedback is very convenient to provide precise radial positioning of the plasma.

Most devices use water cooled copper toroidal field coils but for very high toroidal fiels the required current density can only be obtained using liquid nitrogen cooled copper. A disadvantage of these cryogenic systems is the cool down time between shots. A superconducting tokamak is already in operation in the Soviet Union and here the most difficult thing is the shielding of the superconductor against pulsed poloidal fields. The principal engineering problems in building tokamaks have come from the large magnetic forces involved which principally arise from the high toroidal magnetic fields and the torque on the coils due to interaction with the vertical magnetic field.

The vacuum vessel is usually of corrugated stainless steel which is very often bakeable. Inside this is a limiter of refractory material such as tungsten or molybdenum though carbon and titanium are now more popular. This is used in a tokamak to prevent damage to the thin vacuum vessel by the plasma or the presence of a beam of runaway electrons.

To give some idea of the range of tokamak devices now in operation Fig.7 shows to scale the cross sections of some of the devices in operation which range in physical size from Alcator to DIII. Figure 8 shows the small air-cored basic physics tokamak - TOSCA at Culham and Fig.9 shows the larger DITE tokamak at Culham which is iron-cored and has liquid nitrogen cooled copper coils and neutral injection for additional heating. Figure 10 shows the PLT device at Princeton, USA. This is air-cored and has water cooled copper toroidal field coils and very high power neutral injection for additional heating.

5 OHMIC HEATING EXPERIMENTS

The plasma current in a tokamak heats the plasma resistively to electron temperatures typically of 1-2 keV. Electrons in the interior lose their energy by heat diffusion and convection and by radiation cooling and by equilibration with the ions. These in turn lose their energy by conduction, convection and by charge exchange. At the edge of the plasma the heat outflow is conducted to a limiter. Ohmic heating in tokamaks is most effective for high magnetic fields and small sizes, since the current density is then maximised. The most successful devices of this kind are the Alcator devices at the Massachussetts Institute of Technology[7] and the FT device at Frascati[8] which have operated at fields up to 9T with plasma currents of several hundred kA and plasma radii of 10-20 cm. The intense ohmic heating permits an unusually wide range of plasma densities, up to $10^{15}cm^{-3}$ with temperatures for the ions and electrons of about 1 keV. $n\tau_E$ values of the order of $3x10^{13}cm^{-3}s$ have been attained on these devices.

Of particular interest to the progress of tokamaks is whether an empirical scaling for the energy confinement time τ_E can be established from existing experimental data and used to extrapolate to a reactor. Figure 11 shows a scaling law obtained from results from existing devices (Coppi and Mazzucato 1979)[9] and demonstrates that the confinement time varies approximately linearly with the average density and the square of the minor radius. The simple energy confinement scaling $\tau_E \propto \bar{n}a^2$ provides a reasonably good fit to the experimental data from many experimental devices. Unfortunately numerous other scaling laws for the electron heat conduction have also been shown to produce equally good empirical fits. The scaling laws from early Soviet work show a dependence on plasma current and size; later scaling laws indicate a dependence on the streaming parameter (the ratio of drift speed to sound speed). A systematic analysis has been carried out[10] which assumes that the containment time can be expressed in a form $a^{\alpha}\ b^{\beta}\ c^{\gamma}$ etc where a b c are various machine and plasma parameters. A similar approach has also been used by Pfeifer and Waltz[11]. It should be noted that ohmic heating with classical resistivity introduces a coupling between the electron temperature and the containment time. Taylor and Connor[12] have considered the limits imposed on the scaling indices $\alpha\ \beta\ \gamma$ etc if it is assumed that the plasma behaviour is determined entirely by plasma physics. This leads to restrictions on the indices. It is only possible to obtain decisive information on the temperature scaling when one can use auxiliary heating at a power level which is comparable with or larger than the ohmic input. Present results seem to indicate that the dependence of the confinement time on temperature is weak. No full explanation of the electron confinement scaling yet exists but there are many theories associated with the anomalous transport as indicated earlier which purport to explain the results.

6 ION HEAT CONDUCTION

A pleasing feature of ohmic and neutral beam heated tokamaks is that the scaling of the ion temperature can be explained in terms of purely classical ion thermal conduction. The ion temperature shows agreement with a formula proposed by Artsimovich[13] and derived by balancing the energy flux from the ions and electrons against ion thermal conduction using the appropriate form of neo-classical diffusion. The formula for the plateau regime is

$$T_i = \text{const}\ (I.B_\phi R^2 n_e)^{1/3} A_i^{\frac{1}{2}} \qquad (3)$$

where A_i is the atomic weight of the ion. Operation at high densities shows that the overall energy confinement does tend toward classical, principally because the electron heat conduction then becomes comparable with the classical ion heat conduction.

7 NON-CIRCULAR CROSS SECTIONS

A number of experiments have been performed with non-circular cross sections to test their predicted theoretical advantages. The equation defining the safety factor q, eq(1), indicates that if the poloidal length is increased the toroidal field may be decreased or the plasma current increased for a fixed value of q and this has been verified experimentally. D shaped plasmas have been produced with height to width ratios, b/a, of up to 2 on the DOUBLET devices, TOSCA and T8. Though these devices have demonstrated some improvement in confinement this may have been due to the increased plasma volume in some cases. No gain in critical beta has yet been demonstrated associated with a D shaped plasma. This is probably necessary for future tokamak reactors and remains a short-term objective to be tested with auxiliary heating. Large elongations, $b/a \lesssim 3$ have been obtained on the DOUBLET configuration, Ohkawa, 1979[14]. This is illustrated in Fig.12 for values of q and plasma parameters similar to those obtained in circular tokamaks.

8 TOKAMAK OPERATING REGIMES

It has been known for a long time that the regimes of tokamak operation are limited. Too low a density usually leads to excessive runaway or to the so-called slideaway regime in which strong turbulence is excited by the large ratio of electron drift to thermal speed. Too high a density leads to disruption as also does too low a value of q. The density at which disruption occurs has been shown to scale with the parameter B_ϕ/R which is a measure of the current density on axis as $q \cong 1$ or alternatively roughly proportional to the ohmic input power. Discharge cleanliness is also an important parameter as has been shown by gettering the torus wall with titanium. This can increase the density limit considerably. The results obtained from a number of experiments are shown in Fig.13 in a normalised way, with 1/q as a function of $\bar{n}R/B_\phi$. The high density limit with and without gettering is shown by the two right hand curves; the lower curve, which essentially shows the maximum density that can be obtained for a given current, is not only a property of tokamaks and Fig.14 shows the variation of the maximum line density that can be obtained for ohmic heated devices as the current is varied from 1 kA to 2MA. This proportionality is clearly illustrated. These observations are consistent with a model of disruption in which the ohmic heating is insufficient to prevent cooling of the plasma edge which leads to a contraction of the column, q at the boundary decreases and the gradient of current density increases leading to MHD instability and disruption. When the ohmic heating is supplemented by auxiliary heating, one would expect the critical density to increase and this is indeed observed to be the case.

The upper curve in the operating regime is associated with too low a value of q at the limiter. This is typically in the region of $2.1 \rightarrow 2.5$ with careful

control of the density and plasma current. However on some devices where there is a conducting shell very close to the plasma it is possible to operate with a value of the safety factor q at the limiter of less than 2 e.g. on DIVA[15], T11[16] and TOSCA[17]. This type of operation however appears to be difficult to obtain - in particular the requirements for breaking through the q=2 disruptive barrier.

The inaccessible region to the left which is connected with runaway or slideaway can however be circumnavigated by preionisation and using a low loop voltage. There is also some evidence that pellet refuelling allows the high density limit to be moved somewhat to the right on the figure[18].

9 FLUCTUATIONS IN TOKAMAKS

Early evidence of fluctuations in tokamaks was obtained by Mirnov[19] using magnetic pick-up coils outside the plasma column. Figure 15 shows a typical set of results which show the evolution of n=1, m=6, 5, 4 ... perturbations+ as the current increases and the safety factor at the limiter falls below these values. These are interpreted as the external manifestation of tearing modes centred on the resonant surfaces q = m/n inside the plasma. Figure 16 shows a detailed comparison of the measured magnetic field perturbations, for a mode with m=3, obtained by inserting a magnetic probe into the plasma when compared with theoretical predictions using the measured current distribution and conductivity. This confirms in detail the tearing mode origin of these fluctuations.

Striking evidence of internal fluctuations is obtained from soft x-ray measurements[20]. A typical result is shown in Fig. 17. The signal consists of two parts:-the main oscillation consists of an m=0 mode referred to as a "sawtooth" and a high frequency part due to an n=1, m=1 tearing mode. It is believed that the value of q in the centre of the plasma is limited to about 1 so that when q is driven to less than 1 by ohmic heating an internal instability appears, which manifests itself as the growing oscillation shown in the figure. The figure also indicates the possible evolution of the magnetic surfaces obtained from nonlinear calculations[21] which can reproduce the sawtooth behaviour. The rise in signal is due to ohmic heating and the sudden drop is associated with the internal reconnection produced by the growing tearing mode. The detailed structure of the m=1 mode can be obtained with soft x-ray detectors and compares well with theoretical predictions.

As the value of q decreases towards 2 then large amplitude oscillations of the m=2 mode are observed and are usually followed by a disruptive instability which results in a large negative voltage spike and a substantial reduction in energy content of the plasma and a rapid movement inwards of the plasma. The final phase

+ *m is the poloidal mode number and n the toroidal mode number associated with a perturbation of the form* $e^{i(m\theta+n\phi)}$.

of the instability is an abrupt expansion of the temperature and current profile which can terminate the plasma current and damage the walls of the containing vessel. Disruption appears to be linked with coupling between modes of different helicity. For example in some cases there is a strong coupling between the m=1 internal mode and the m=2 mode. Probe measurements show that large magnetic islands are formed shortly before disruption and these become so large that the magnetic surfaces break as shown in Fig.18. One model of the disruption is that these m=2 islands become so large that they interact with the limiter and cool outer regions of the plasma forcing the current channel to shrink which induces other instabilities to grow and produce a disastrous reduction in the energy content of the plasma. In some situations a coupling between the m=2 mode and the m=3, n=2 mode is observed and this can grow very rapidly as shown in Fig.19. When the two sets of magnetic islands become sufficiently large, the magnetic surfaces are destroyed and a disruption may result. This form of disruption has been demonstrated experimentally[22] and is the basis of the nonlinear calculations of Waddell et al[23]. As an example Fig.20 shows the distorted flux surfaces calculated from the measured perturbations shortly before disruption when both large magnetic islands and ergodic field line behaviour are indicated.

It has been shown that it is possible to trigger disruptions with the addition of helical windings with m=2, n=1[24]. The artificially created islands may also have a stabilising effect and permit hard disruptions to be avoided. The only clear situation in which the disruption can be avoided is on stellarator-like devices where a significant rotational transform is present. There is probably no unique form of mode-coupling which ultimately produces disruption. It is likely that this is a manifestation of the plasma relaxing to a state of lower magnetic energy[25].

The disruption nevertheless represents a serious obstacle to large tokamaks and reactors, since it can yield large transient voltages, induce substantial mechanical forces and produce large thermal loads on the first wall.

Measurements of density fluctuations by microwave scattering and by CO_2 laser scattering have been made on a number of devices. However, having measured the level of fluctuations and the frequency spectrum, the major difficulty is to relate this to the plasma loss rate. Much more work is necessary to establish any correlation between density fluctuations and energy transport.

10 ADDITIONAL HEATING

Ohmic heating is unlikely to produce reactor temperatures in future large machines as the resistivity of a plasma decreases rapidly with increasing temperature.

A plasma at 10^7°K (= 1 keV) has about the same resistivity as room temperature copper.

Transient heating of a tokamak by adiabatic compression in two and three dimensions has been successfully demonstrated on the ATC[26], TOSCA[27] and TUMAN[28] experiments. Magnetic compression in minor radius as on the TOSCA and TUMAN devices has been achieved by raising the toroidal field on a short timescale ($\sim$ 500 μs) comparable to the energy confinement time on these devices. This is found to be quite successful at heating the plasma; in particular, the heating is found to be greater than that associated with an adiabatic compression probably because of the detachment of the plasma from the surrounding boundaries. Unfortunately considerable power is required to increase the toroidal field and a more elegant scheme is to decrease the major radius using an increasing vertical field. This increases the toroidal field around the plasma without increasing the current in the toroidal field coils. The ATC device at Princeton, USA, utilised such a compression and was able to achieve a threefold increase in the value of beta in this way. Apart from its transient nature this method of heating suffers from the inefficient use of the toroidal field coils.

The most effective heating method that has been applied to tokamaks is the injection of powerful beams of neutral atoms which become trapped in the form of circulating thermal ions, the ions thermalising gradually with the bulk plasma ions. Power levels of up to 6 MW have already been used with a typical injection energy of 40 keV which is an order of magnitude higher than the plasma energy, and the particle influx due to the beam may be smaller or even comparable to the particle loss rate from the plasma. The mean free path for the ionisation of the neutral beam in the plasma is typically of the same order as the plasma radius. This ensures a broad distribution of the heating effect over the plasma volume together with a high absorption efficiency for the incoming beam. The most successful experiment to date has been the Princeton Large Torus (PLT) where neutral injection powers of 2.4 MW raised the temperature to 6.5 keV[29]; this is shown in Fig.21 This temperature is comparable to the minimum ignition temperature for a D-T reactor. In these neutral beam heated plasmas the collisionality is about the same as in a reactor and yet the ion thermal conduction continues to agree with classical theory within the error of measurement. The electron thermal conductivity is found to decrease with rising electron temperature in the central regions of the plasma.

In ohmic heated tokamaks, the volume average value of beta can approach about 1% and yet a value of at least 5% is desirable in a commercially attractive power reactor. Several devices have now been able to obtain values of beta up to 3% by

means of intense neutral beam heating. The ISX device at Oak Ridge[30], T11[16] at the Kurchatov Institute in Moscow, and the JFT-2[31] device in Japan have all reached values of approximately 3% in relatively low field tokamak regimes. These results have been encouraging because the theoretically predicted stability limits for the experiments ($R/a \sim 4$, $q \sim 3$ and in a circular cross section) are about 2%. However at the highest beam powers in these experiments there is deterioration in confinement which may be the result of poor confinement at high beta or that high beam powers may induce undesirable effects in the plasma. Continuing studies are required to obtain the critical beta values in various geometries, in particular the D shaped cross section plasmas.

A variety of radio frequency heating methods is being investigated, which match the frequency and wavelength of the driving field to a natural mode of oscillation in the plasma thus exciting a coupling resonance. At the present time, successful heating of the electrons at the electron cyclotron frequency using gyrotrons of frequency 28 → 86 GHz has already been demonstrated in a number of tokamaks, with high efficiency.[33] Heating has also been investigated at the cyclotron frequency of a 'minority' ion species. Recent experiments of this kind have generated minority ion populations in the 10 keV range which have thermalised with the bulk ion population to give increases in the ion temperature in excess of 1 keV[32]. The efficiency of radio frequency heating and the best neutral beam heating experiments are comparable.

11 CURRENT DRIVE

The circulating fast ions produced by injection form a current I_f but collisional momentum transfer to the plasma electrons generates an opposing electron current I_e. The net current, $I_{bd} = I_f - I_e$, is driven by the beam and not the transformer consequently it can in principle permit continuous operation of a tokamak[34]. As the transformer circuit on many devices maintains the current constant, the beam driven current manifests itself as a change in loop voltage from the transformer, V. Figure 22 shows the change in voltage and the comparison between the deduced beam driven current and that predicted theoretically for the DITE tokamak[35]. It is also possible to drive the plasma current using radio frequency waves. This has been demonstrated on small scale experiments using electron cyclotron heating[36]. It has also been demonstrated in lower hybrid heating experiments[37] and in a very impressive way on the PLT device at Princeton. In this case 60 kW of radio frequency power was sufficient to maintain a current of 400 kA for a second.

12 PLASMA FUELLING

The injection of fresh fuel into a toroidal reactor has long been envisaged in terms of high velocity D-T, ice pellets, which are supposed to evaporate and turn into plasma after penetrating into the plasma interior. There has however been considerable uncertainty in respect of both the plasma penetration process itself and the possible effect of a highly localised density perturbation on the quality of tokamak confinement. These concerns have been alleviated considerably by the successful injection of mm sized high velocity D-T ice pellets moving at 10^5cm/s [38]. Even though the mean plasma density can be more than doubled by the pellet injection process, the gross energy content and stability of the discharge have been maintained throughout the refuelling process. Plasma start up has also been achieved using large pellets on DOUBLET III [18].

13 IMPURITY CONTROL

One of the biggest threats to achieving ignition is the presence of even very small concentrations of heavy impurity ions which may evolve from the vacuum chamber wall and limiter. One solution to this is to use a divertor which channels the escaping plasma magnetically in to a chamber separate from the main torus with a high pumping speed to remove impurities. A divertor may be created using the poloidal field or the toroidal field or a bundle type in which a bundle of flux lines is extracted from the torus. These divertors are indicated schematically in Fig.23. Plasma diversion and a reduction in radiative power from impurities in the plasma have been demonstrated on the DITE, PDX and ASDEX devices. It is found in particular on the large poloidal divertor experiment, PDX, that the control and optimisation of the plasma is greatly facilitated by the divertor mode of operation. An interesting result is that most of the plasma loss is found to occur from the outside of the magnetic surfaces, as is evidenced by the target plates in the divertor chamber which receive the escaping particles and energy.

It may be that simpler means of controlling impurities are possible without the necessity for the increased magnetic volume necessitated by a divertor. For example, incorrect limiter material can result in almost all the input energy being radiated away. The use of graphite limiters can avoid significant radiation problems since the carbon ions are completely stripped in the plasma interior. Other approaches such as a pump limiter are currently being considered.

14 FUTURE DEVICES

The consistent pattern of results from tokamaks throughout the world has given confidence that near reactor conditions can be achieved in the next generation of tokamak experiments. There are four such machines under construction in the world, JET in Europe, T15 in the USSR, TFTR in the USA and JT60 in Japan. All are

due to begin operation in the mid-1980s.

The T60 device in Japan is designed to operate with a plasma current of up to 3 MA in a circular plasma in hydrogen. An axisymmetric divertor is included which will facilitate plasma wall interaction studies, and impurity control.

The TFTR project in the USA concentrates on generating fusion power densities of reactor relevance $\sim$ 1 W/cm^3. The emphasis is on the beam-target mode of operation with tritium. There will be a 5 keV target plasma and a 120 keV beam.

The T15 device in the Soviet Union concentrates on superconducting toroidal field coils and radio frequency heating of the plasma.

The objective of the JET experiment is to obtain and study plasma under conditions and dimensions which approach those needed in a fusion reactor. The toroidal vacuum vessel has a major radius of 3 m and a D-shaped cross section of radii 2.1 m vertically, and 1.25 m horizontally. The plasma current will be between 2.6 and 4.8 MA. A key objective is operation in conditions where alpha particles from deuterium-tritium reactions are produced and a study of the subsequent plasma interaction and heating. Figure 24 shows a cross section of the JET apparatus. The vacuum chamber is composed of a series of thick box sections and bellows and is made from Inconel. The toroidal field magnet is formed by 32 coils which are D-shaped to reduce stresses. A mechanical shell withstands the torque which arises when the poloidal field crosses the toroidal field coils. The poloidal field coils are connected in parallel to simulate a copper shell to assist in stabilising axisymmetric deformations or displacements of the plasma. The poloidal field coils around the central magnetic core create the primary flux and the central section of the core is driven far into saturation. Neutron production, from D-D and D-T discharges and hard X-rays which can be produced, requires a 2.5 m thick concrete shield.

These experiments will give a realistic assessment of the potential of the tokamak system and will provide the design parameters of the next stages of development such as the INTOR, NET and FED devices.

15 CONCLUSIONS

Regarding future experimental work, key issues are:-

(1) The need to establish the parametric variation of cross-field electron heat conduction to enable a comparison with theory to be made.

(2) The development of auxiliary heating techniques.

(3) The application of strong additional heating to test beta limits and confinement scaling and to vary the current density profile.

(4) The testing of divertor concepts.

(5) Developing means of controlling and minimising the effects of disruptions.

(6) Developing means of current drive to make continuous operation of a tokamak possible.

(7) The construction and commissioning of multi megamp devices to obtain near ignition conditions.

Outstanding theoretical problems are

(i) Understanding the disruptive instability

(ii) Understanding cross-field thermal conduction

(iii) Understanding beta limits

(iv) Understanding particle diffusion, in particular the behaviour of impurities

(v) Developing methods of current drive.

There has been widespread and rapid progress in controlling and confining high temperature plasmas over the last ten years. In tokamaks it is now routine to sustain plasmas with temperatures of 10^{7}°K for times of 1 second. Energy confinement times of 1/10th of a second can be obtained and the Lawson product, $n\tau_E$, values are within a factor of ten of those which are needed in a D-T ignition system. The next large devices will come into operation in the early 1980's and are aimed at closing the remaining gap. The next few years promise to be particularly exciting in the development of the tokamak. The solution of the remaining practical problems calls for a number of new inventions and advances in our understanding and at a level of creativity comparable to or greater than that in the past. The level of expenditure will be considerably larger and the prospects of ultimate success seem increasingly favourable.

February 1982
DCR/CMS/23

REFERENCES

[1] Bezbatchenko A L et al, Atomn. Energy 1 26,(1956). (UCRL-Trans-307(L)).

[2] Peacock N J, Forrest M J, Robinson D C, Wilcock P D and Sannikov V V, Nature, 224, 488 (1969).

[3] Bennett W H, Phys.Rev. 45 890 (1934).

[4] Clarke J F, Oak Ridge National Laboratory Report, ORNL/TM 5429 (1976).

[5] Tamm I E, Plasma Physics and the Problem of Controlled Thermonuclear Reactions, Pergamon Press 1 35 (1961).

[6] Pfirsch D and Schluter A, Max-Planck Inst. Munich, MPI-PA7 62.

[7] Gondhalekar A et al, Proc. 7th Int. Conf on Plasma Physics and Cont. Nuclear Fusion Research (Innsbruck 1978) 1, 199 (IAEA Vienna 1979).

[8] Bartiromo R et al, Proc. 8th Int. Conf. on Plasma Physics and Cont. Nuclear Fusion Research (Brussels 1980) 1, 43, (IAEA Vienna 1981).

[9] Coppi B and Mazzucato E, Phys.Letts. 71A, 337 (1979).

[10] Hugill J and Sheffield J, Nuclear Fusion 18, 15 (1978).

[11] Pfeifer A and Waltz R, Nuclear Fusion 19, 51 (1979).

[12] Taylor J B and Connor J W, Nuclear Fusion 17, 1047 (1977).

[13] Artsimovich L A, Nuclear Fusion 12, 215 (1972).

[14] Ohkawa T, Proc. 9th Euro.Conf. Plasma Physics and Cont. Nuclear Fusion, (Oxford 1979) 2, 321.

[15] Maeda H et al, Proc. 7th Int. Conf. on Plasma Physics and Cont. Nuclear Fusion Research, (Innsbruck 1978) 1, 377, (IAEA Vienna, 1979).

[16] Leonov V D et al, Proc. 8th Int. Conf. on Plasma Physics and Cont. Nuclear Fusion Research (Brussels 1980) 1, 393, (IAEA Vienna, 1981).

[17] Ellis J J et al, ibid, 1, 731.

[18] Marcus F B et al, Nuclear Fusion 21 859, (1981).

[19] Mirnov S V and Semenov I B, Atomn. Energy 30, 14 (1971).

[20] von Goeler S et al, Phys.Rev.Letts 33, 1201 (1974).

[21] Sykes A and Wesson J A, Phys.Rev.Letts, 37, 140 (1976).

[22] McGuire K M and Robinson D C, Phys.Rev.Letts, 44, 1666 (1980).

[23] Waddell B V et al, Phys.Rev.Letts. 41 1386 (1978).

[24] Karger F et al, Proc. 5th Int. Conf. Plasma Physics and Cont. Nuclear Fusion Research, (Tokyo 1974) 1 207 (IAEA Vienna, 1975).

[25] Taylor J B, Phys.Rev.Letts 33 1139 (1974).

[26] Bol K et al, Proc. 5th Int. Conf. Plasma Physics and Cont. Nuclear Fusion Research (Tokyo 1974) 1, 83, (IAEA Vienna, 1975).

[27] Cima G et al, Culham Laboratory Report CLM-R213, (1981).

[28] Kaganski M G et al, Proc. 6th Int. Conf. Plasma Physics and Cont. Nucl. Fusion Research, (Berchtesgaden 1976) 1, 387, (IAEA Vienna 1977).

[29] Eubank H et al, Proc. 7th Int. Conf. on Plasma Physics and Controlled Nuclear Fusion Research, (Innsbruck 1978) 1, 199, (IAEA Vienna 1979).

[30] Murakami M et al, Proc. 8th Int. Conf. on Plasma Physics and Controlled Nuclear Fusion Research, (Brussels 1980) 1, 377 (IAEA Vienna 1981).

[31] Suzuki N et al, ibid, 2 525.

[32] Furth H P, Proc. 9th Euro Conf. on Plasma Physics and Controlled Nuclear Fusion (Oxford 1979), 2 309.

[33] Strelkov V S, ibid, 2 387.

[34] Ohkawa T, Nuclear Fusion 10 185 (1970).

[35] Clark W H M et al, Phys.Rev.Letts 45 1101 (1980).

[36] Start D F H et al, Phys.Rev.Letts to be published, or Culham Laboratory Report CLM-P644 (1982).

[37] Yamamoto T et al, Phys.Rev.Letts 45 716 (1980).

[38] Milora S L et al, Phys.Rev.Letts 42 270 (1979).

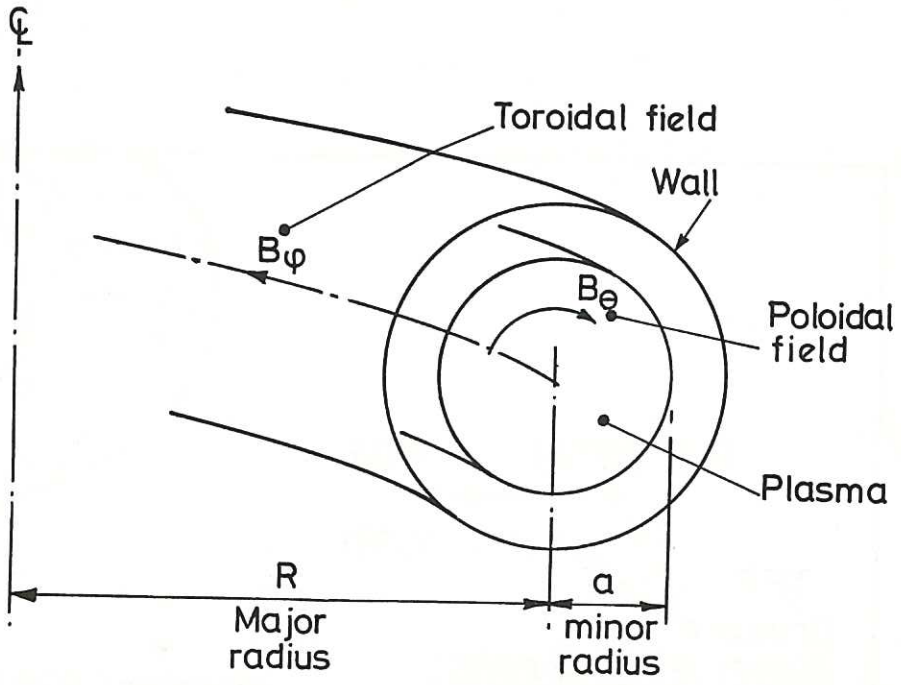

Fig.1 Fields and co-ordinates used to define a toroidal pinch.

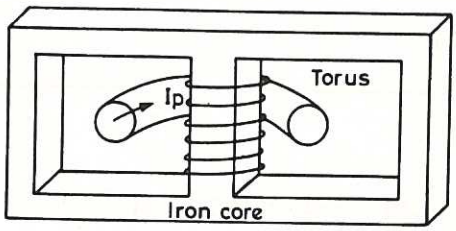

(a) General arrangment

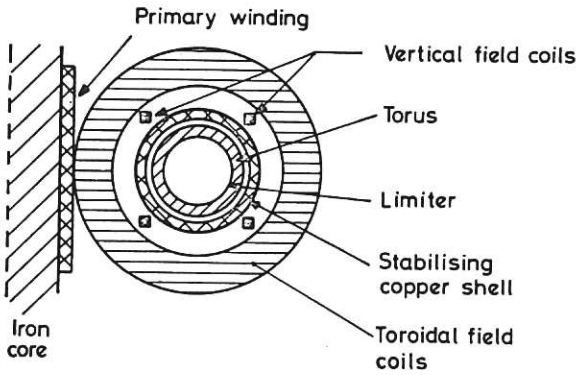

(b) Meridional cross-section

Fig.2 Standard disposition of coils and vacuum vessel for a toroidal pinch.

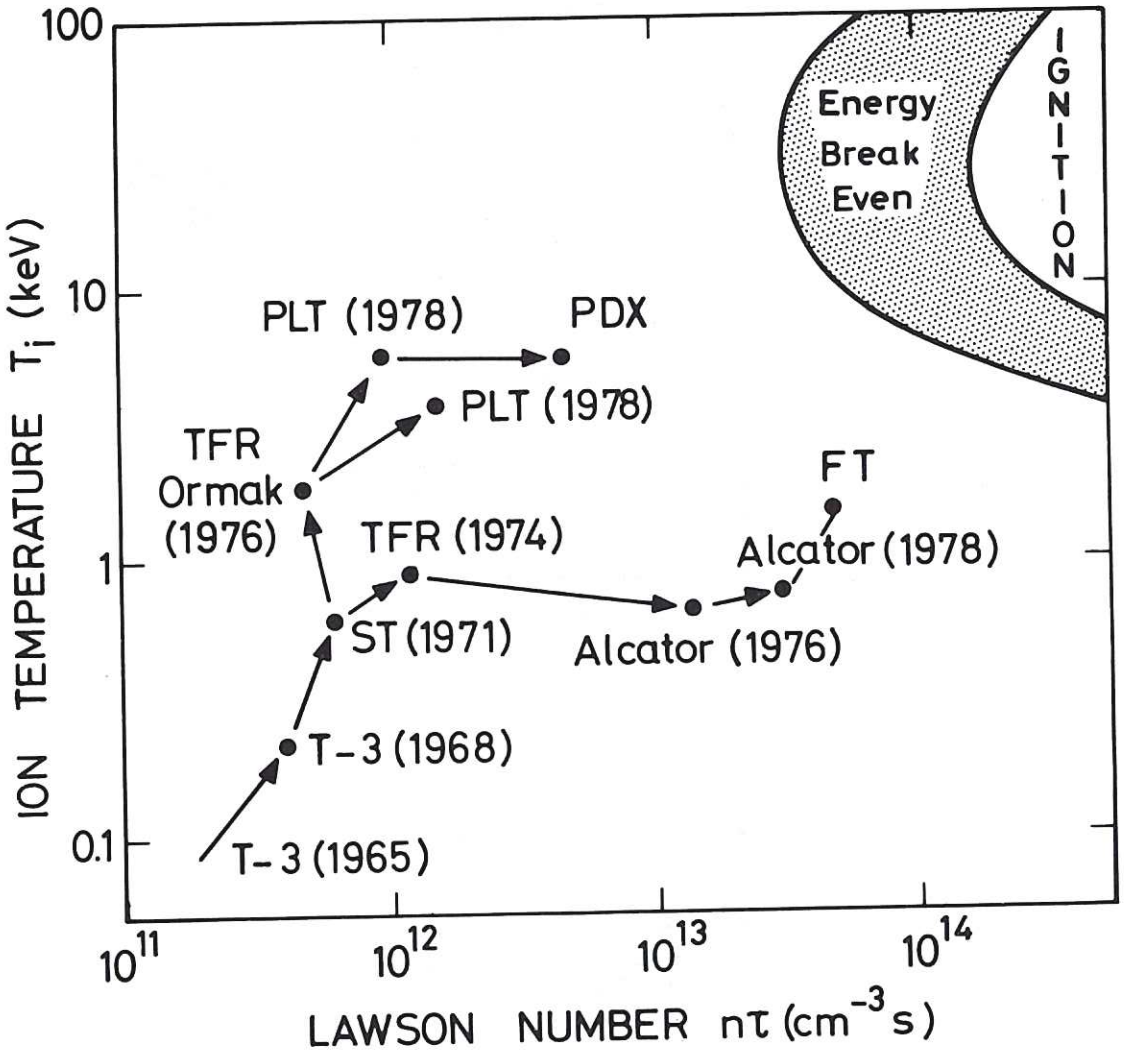

Fig.3 Progress of tokamak experiments towards parameter values of reactor interest.

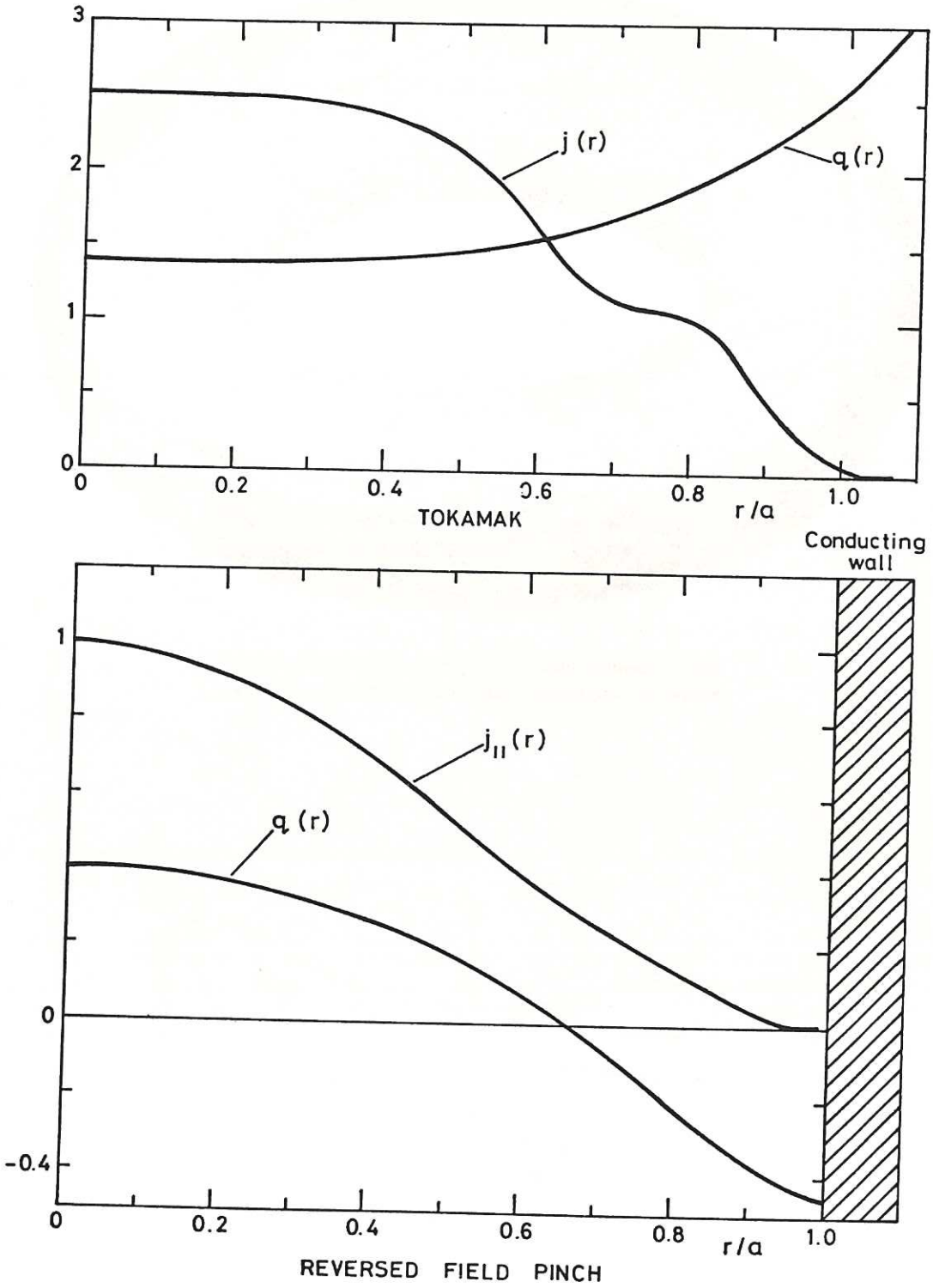

Fig.4 (a) **Stable current distribution for a tokamak, showing the radial variation for the normalised pitch, q(r).**

(b) **Stable parallel current distribution for a reverse field pinch showing the radial variation of the normalised pitch. Here a conducting wall, whose position is indicated, is required to stabilise the pinch.**

Fig.5 Rippled surface of a plasma torus produced by ballooning modes associated with a high value of beta.

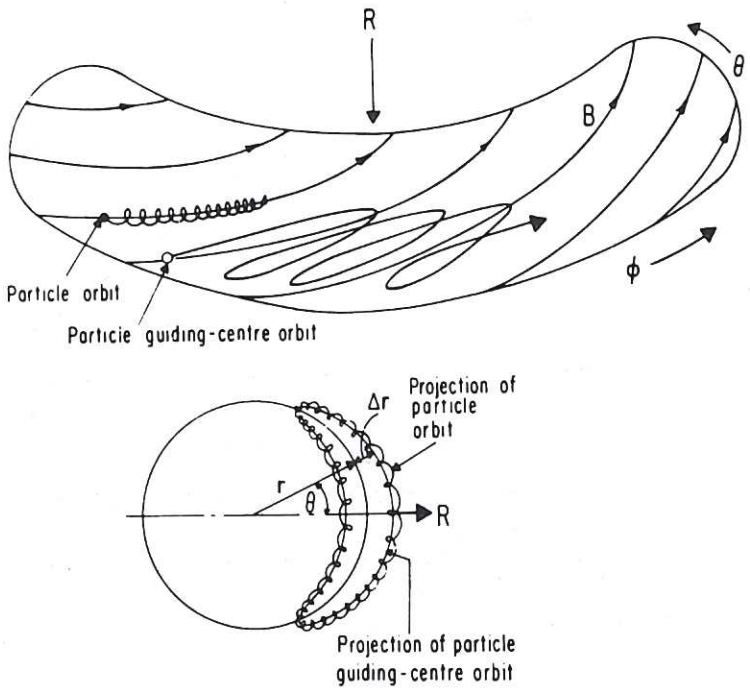

Fig.6 Trapped particle orbit in the tokamak.

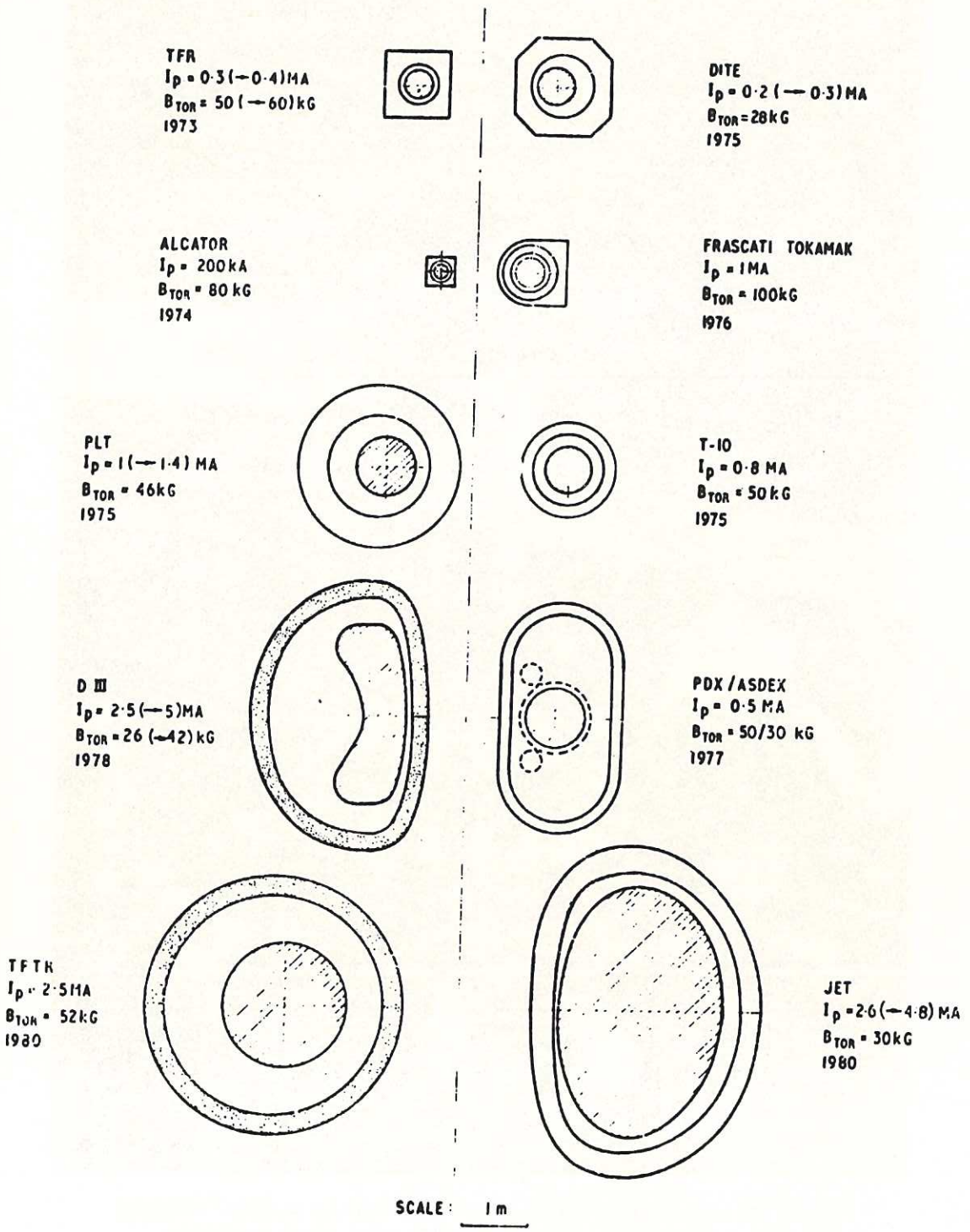

Fig.7 The relative size of the main devices which are at present in operation, under construction or in design through the world. Dimensions are to scale and the plasma current and magnetic field are given in each case.

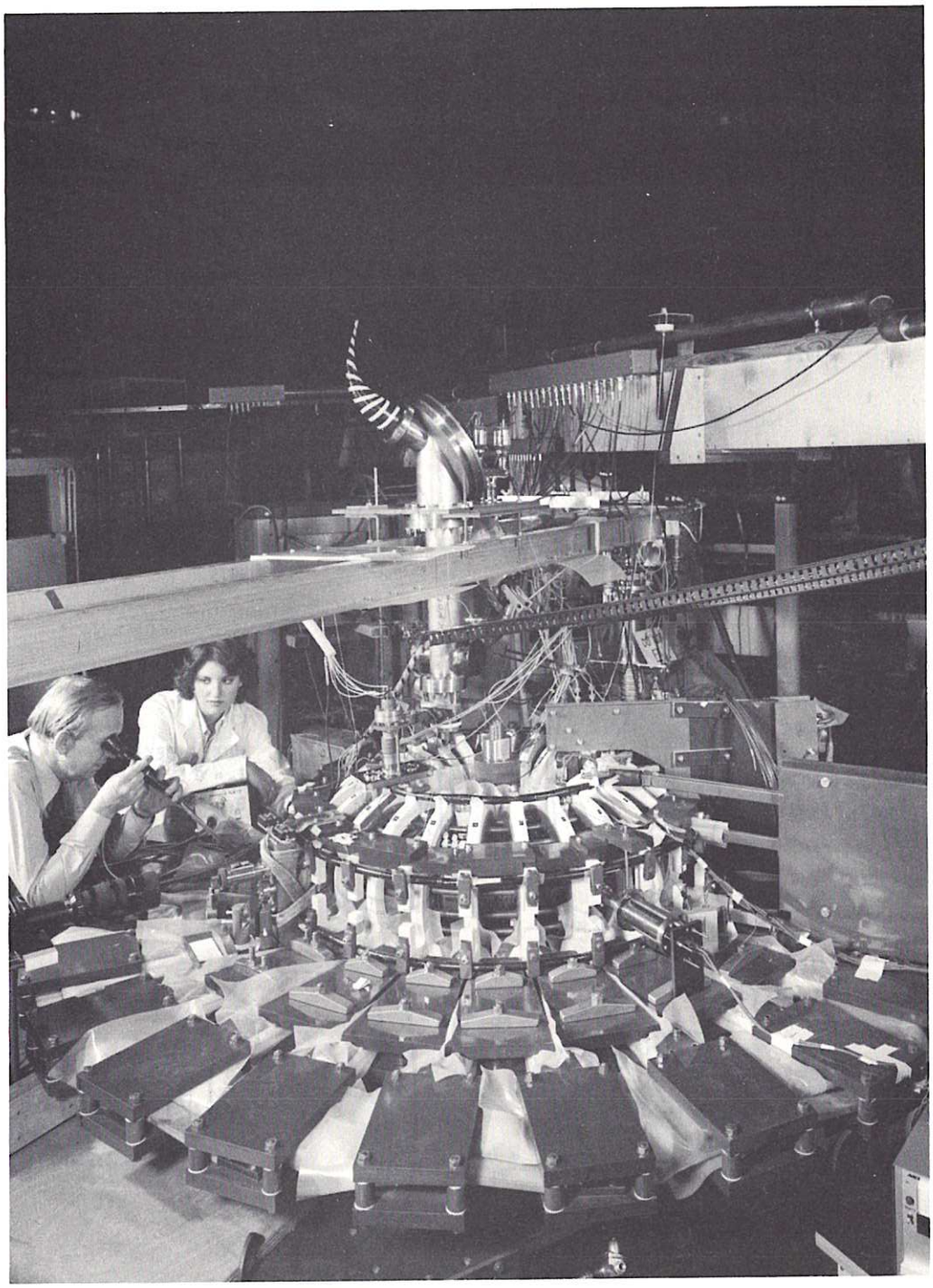

Fig.8 The small tokamak, TOSCA, which is air-cored, has windings for shaping the plasma and single-turn toroidal field coils to permit plasma compression.

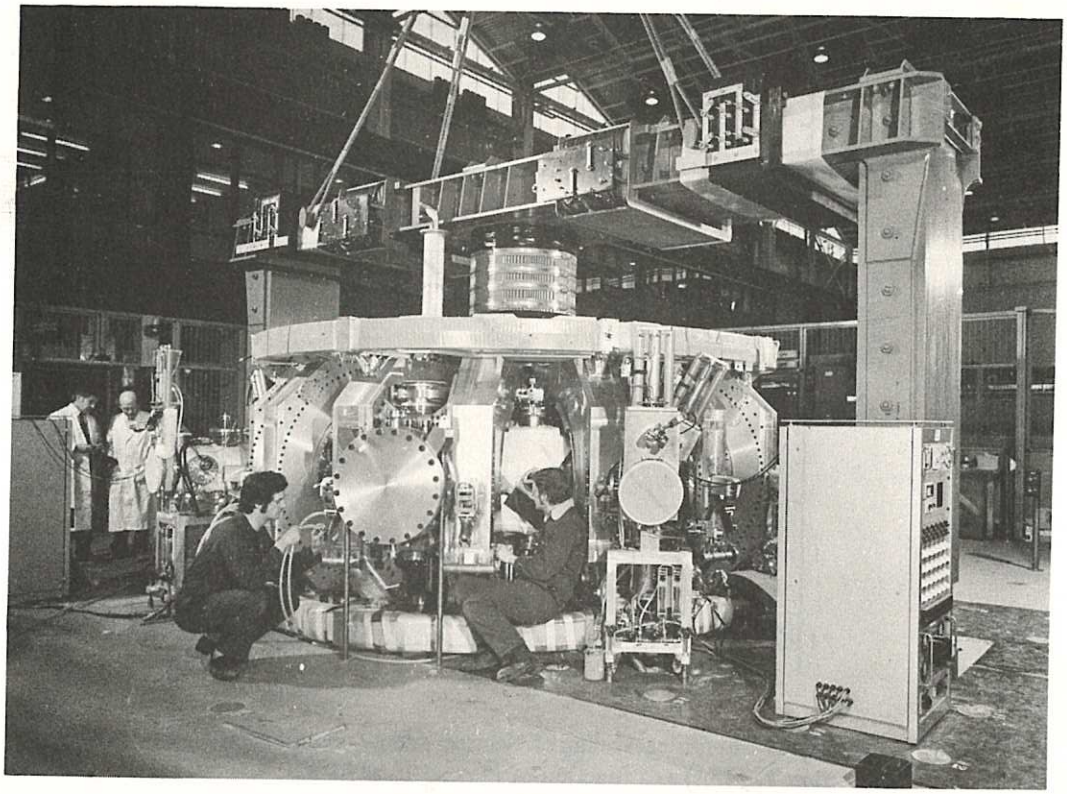

Fig.9 The DITE tokamak which is iron cored has a bundle divertor and neutral injection for additional heating.

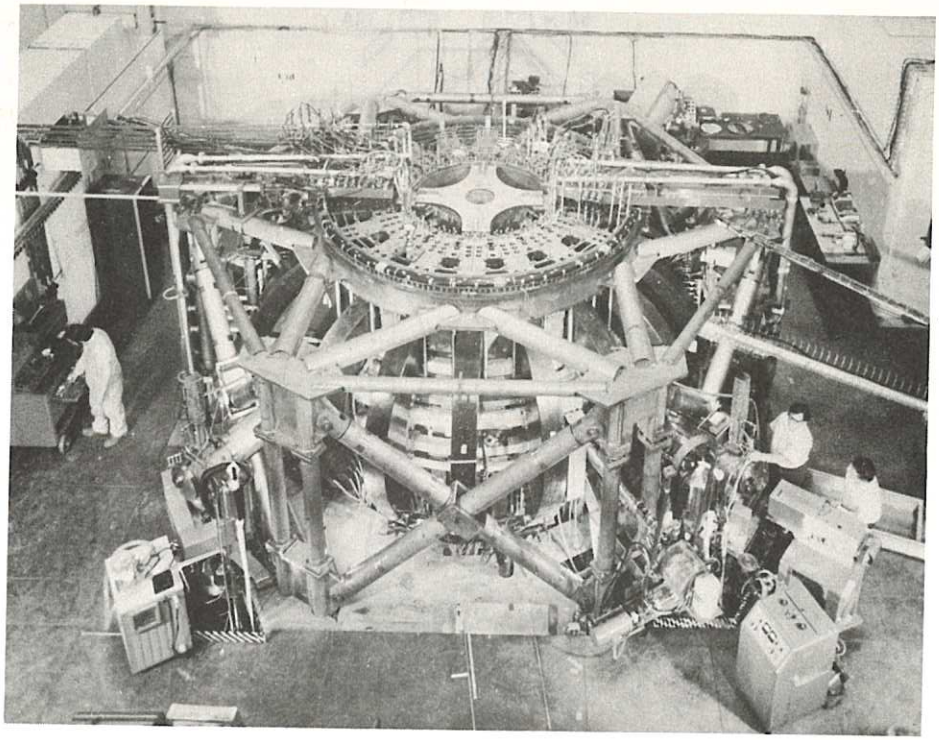

Fig.10 The Princeton Large Torus (PLT) tokamak, which is air-cored, has achieved the highest sustained ion temperatures to date with neutral injection as additional heating.

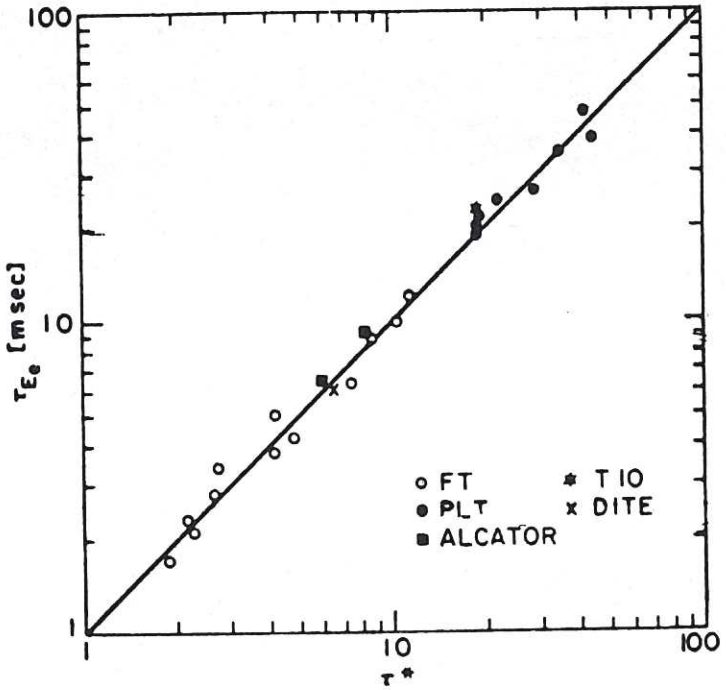

Fig.11 Empirical scaling of electron energy confinement time τ_{Ee} (ms) as a function of $\tau^* \propto n_e T_e a^3/R B_\theta$ showing results from five different tokamaks.

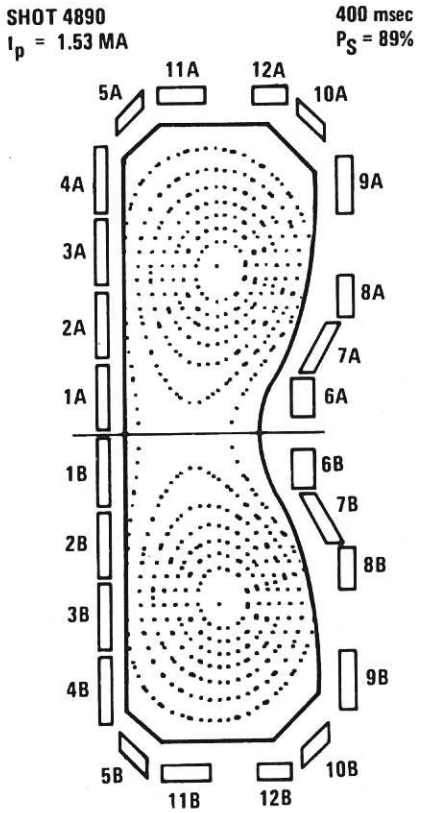

Fig.12 Doublet configuration as measured on the large Doublet III facility at a plasma current of 1.5MA.

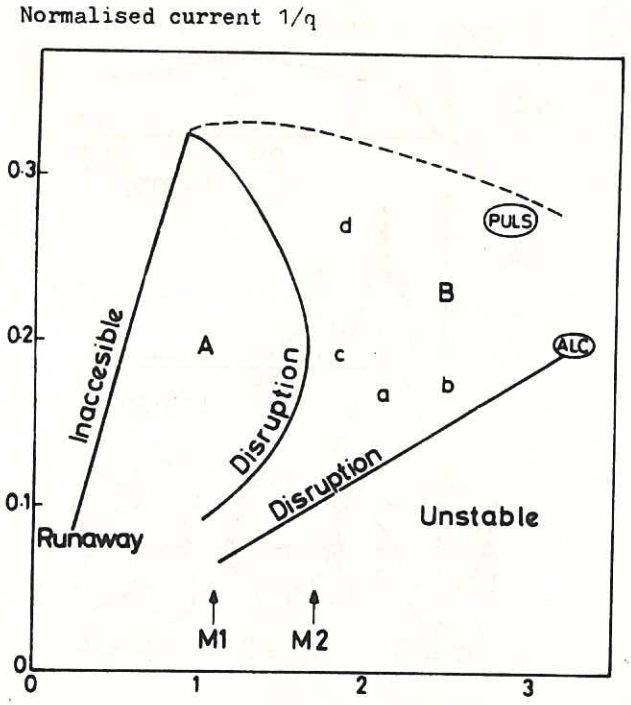

Fig.13 Stable operating regimes in normalised I_p, n_e space for the DITE tokamak.
A without gettering, B with gettering.
M2, M1, density limits in Ormak with and without gas puffing.
ALC, PULS denote operating regimes in Alcator and Pulsator.

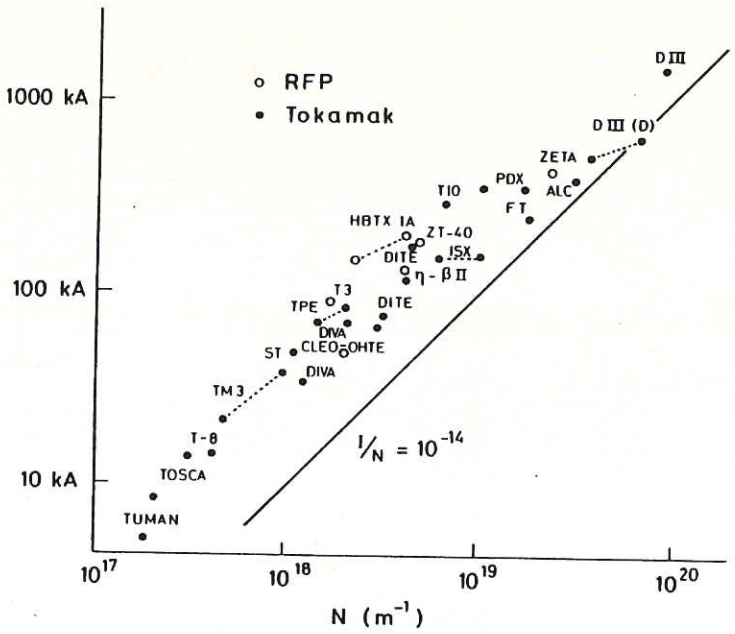

Fig.14 Maximum attainable line density as a function of plasma current for pinches and tokamaks.

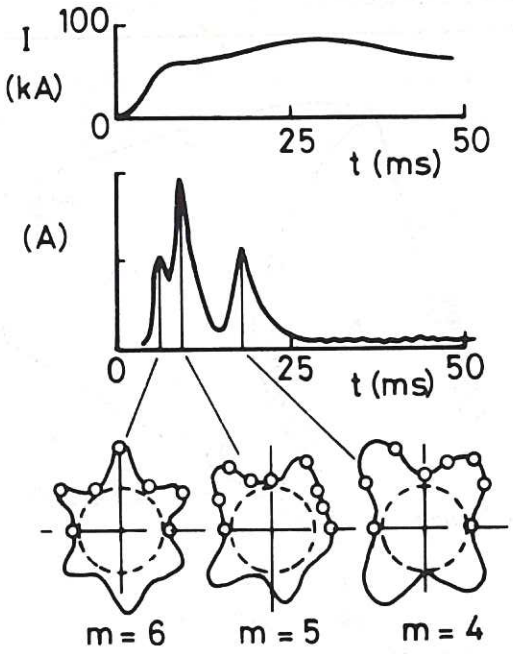

Fig.15 Perturbations in the initial stages of a tokamak discharge. Amplitude A as a function of time and polar co-ordinate at three different times.

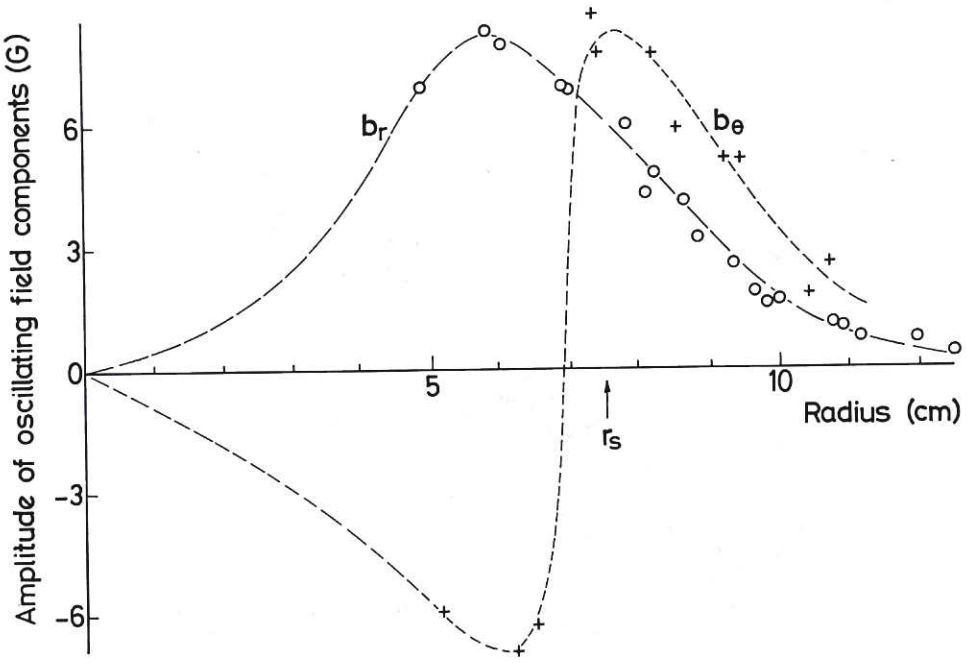

Fig.16 A comparison of the measured radial distribution of magnetic field perturbations, b_r, b_θ observed in the small tokamak TOSCA with those predicted for an m=3 tearing mode by using the measured current distribution and value of S (magnetic Reynolds number = τ_σ/τ_A, where τ_σ is the field diffusion time and τ_A the Alfvén transit time). The radial position at which q=3 is indicated by r_s.

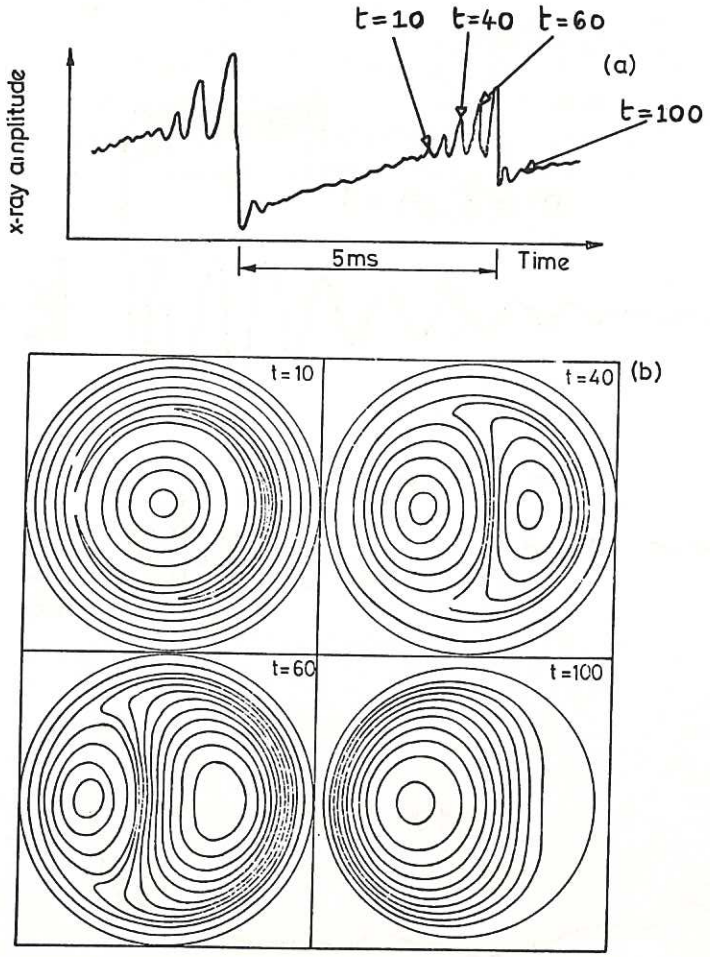

Fig.17 (a) Soft x-ray emission signal as a function of time.
(b) The oscillations correspond to a rotating m=1 mode whose magnetic surfaces give rise to growing magnetic island structures as shown.

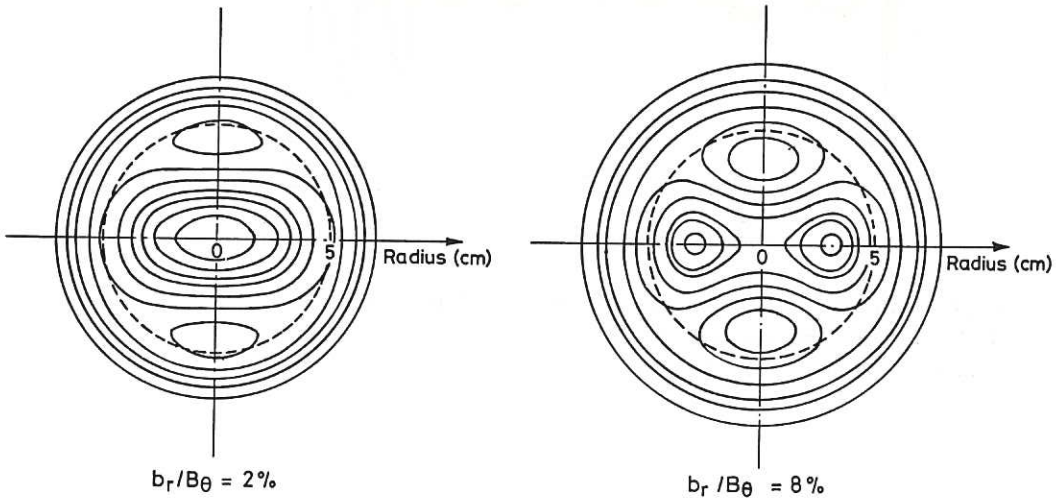

Fig.18 m=2 magnetic islands derived from measurements up to the time of disruption.

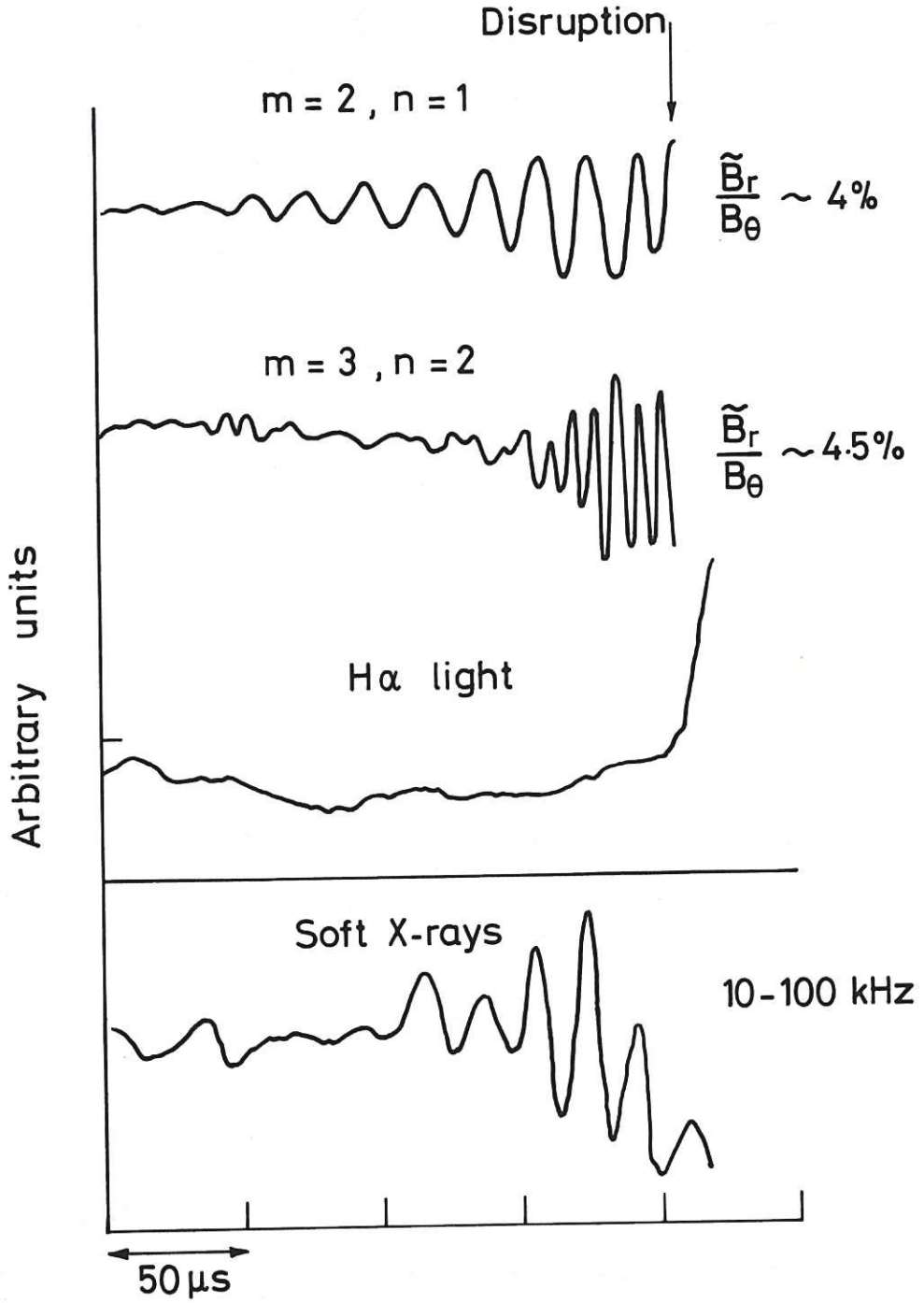

Fig.19 Evolution of the m=2, n=1 and m=3, n=2 modes at a major disruption on the TOSCA device, together with the H_α light and the soft X-ray central channel emission. The arrow indicates the time of disruption.

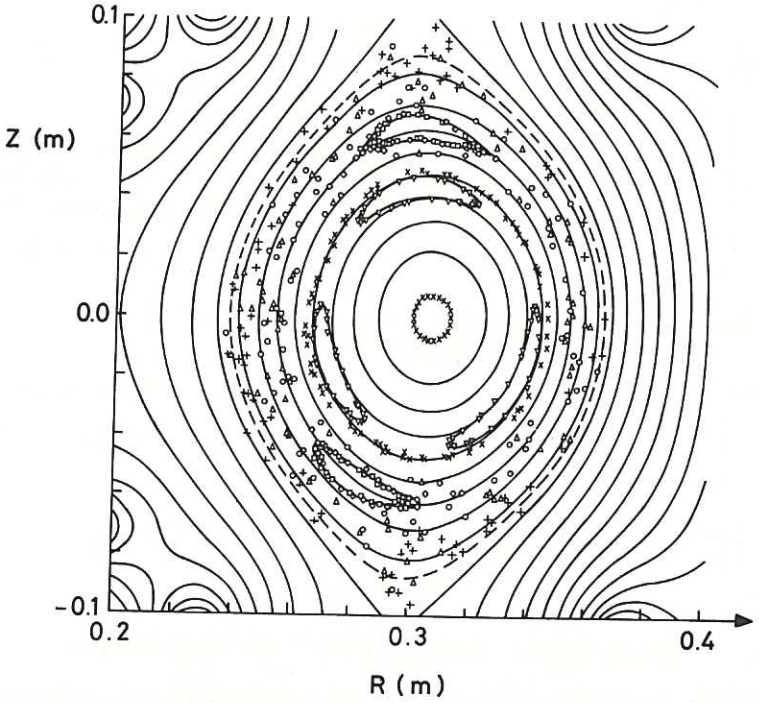

Fig.20 Distorted flux surfaces calculated from measured field perturbations for the m=2, n=1 and m=3, n=2 modes shortly before disruption for an elliptical plasma on the TOSCA device.

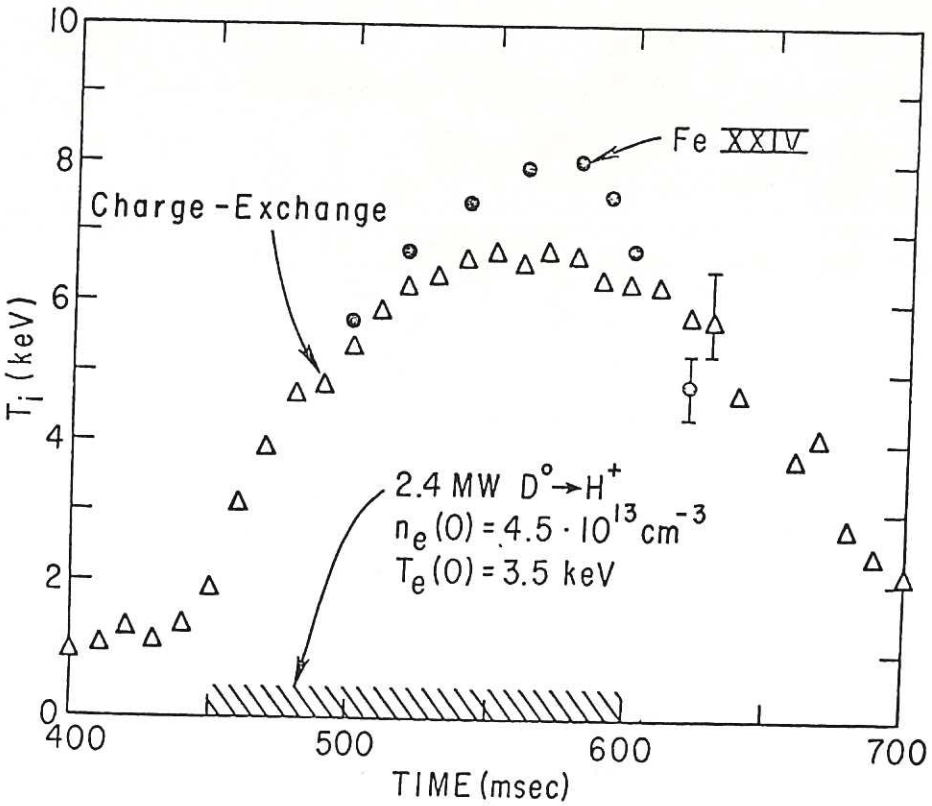

Fig.21 In the course of a PLT ohmic-heating discharge of approximately 1 s duration, neutral beam heating is applied for 0.15 s to raise the ion temperature.

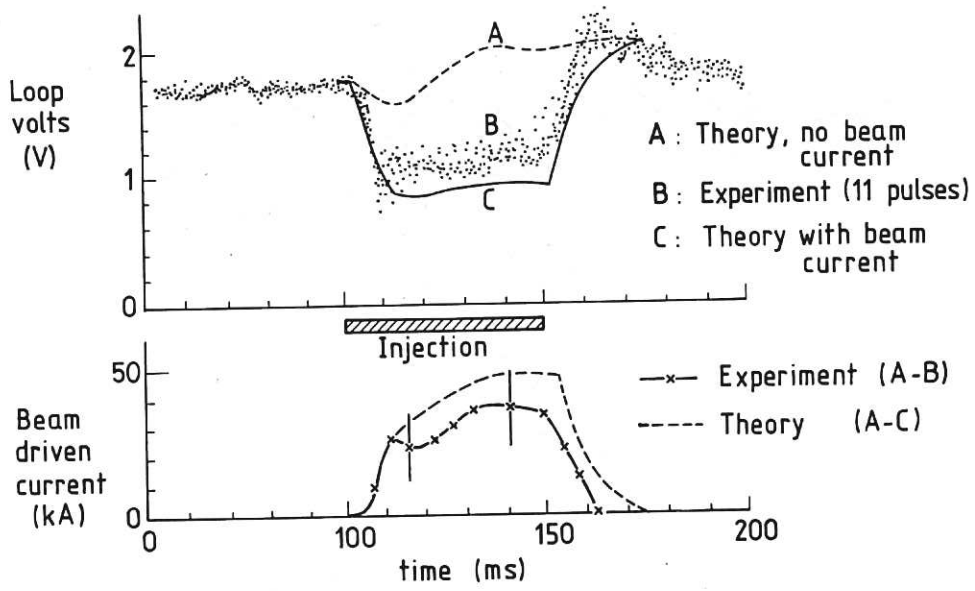

Fig.22 Change in voltage and comparison between the deduced beam-driven current and that predicted theoretically for DITE.

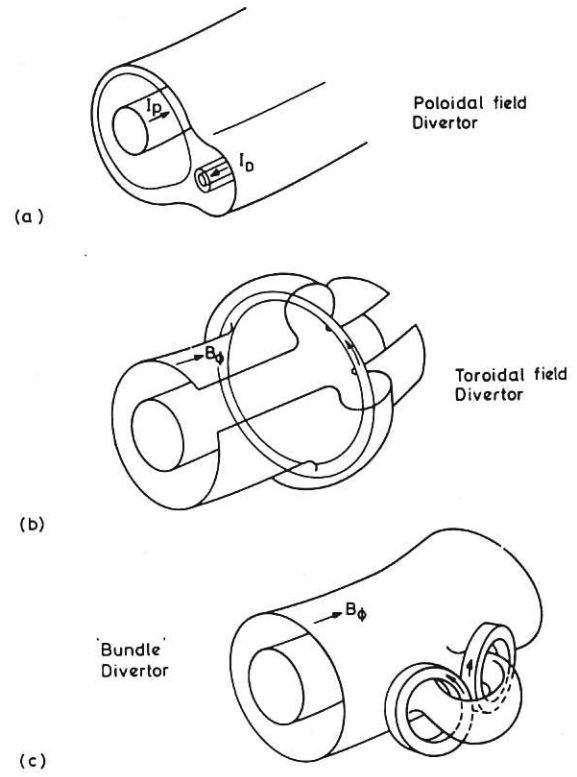

Fig.23 Schematic diagram of various types of divertor.

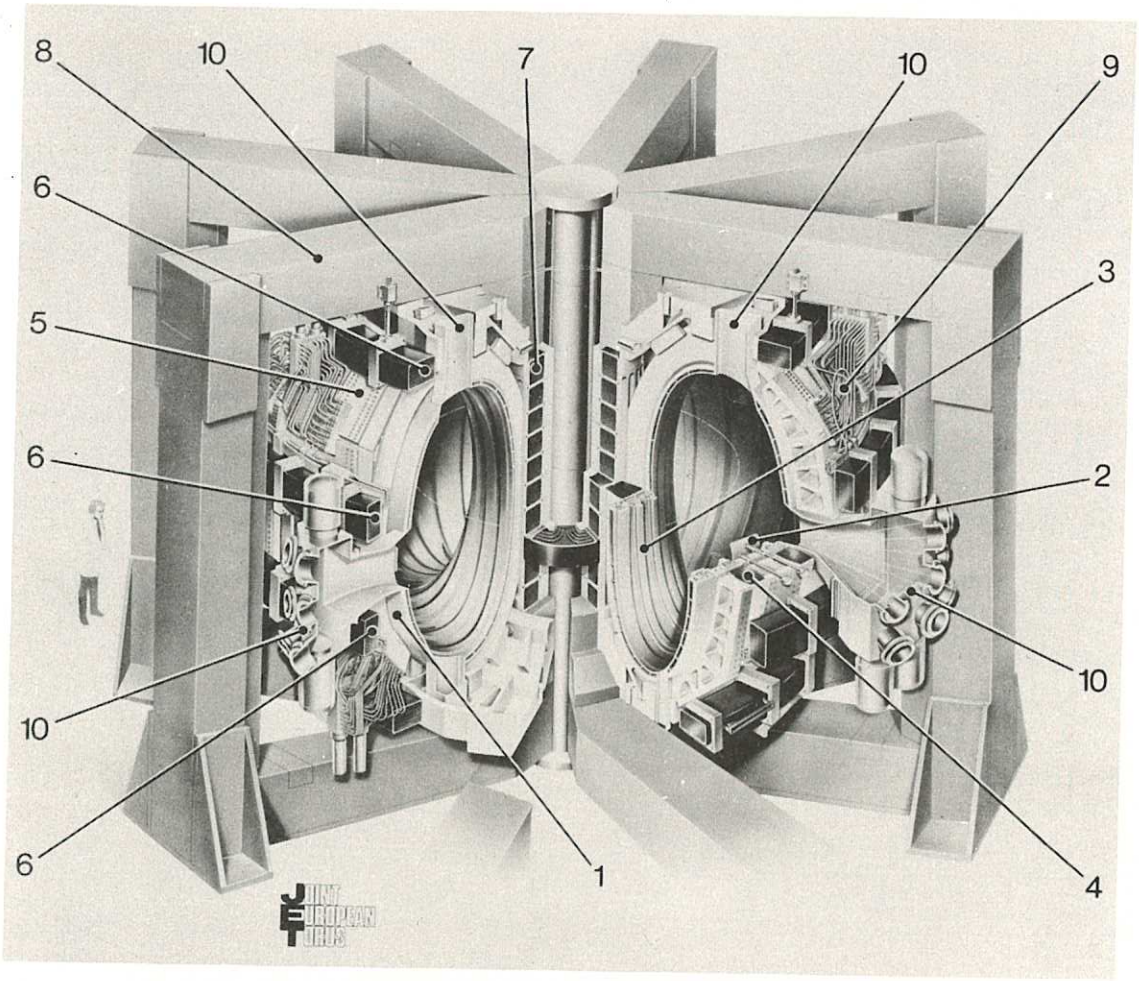

Fig.24 The JET apparatus.

1. Vacuum vessel (double walled)
2. Material limiter defining the outer plasma edge
3. Poloidal protective shields to prevent the plasma touching the vessel.
4. Toroidal field magnet of 32 D-shaped coils
5. Mechanical structure
6. Outer poloidal field coils
7. Inner poloidal field coils (primary or magnetising windings)
8. Iron magnetic circuit (core and eight return sections)
9. Water and electrical connections for the toroidal field coils
10. Vertical and radial ports in the vacuum vessel.

HER MAJESTY'S STATIONERY OFFICE

Government Bookshops

49 High Holborn, London WC1V 6HB
(London post orders: PO Box 569, London SC1 9NH)
13a Castle Street, Edinburgh EH2 3AR
41 The Hayes, Cardiff CF1 1JW
Brazennose Street, Manchester M60 8AS
Southey House, Wine Street, Bristol BS1 2BQ
258 Broad Street, Birmingham B1 2HE
80 Chichester Street, Belfast BT1 4JY

Publications may also be ordered through any bookseller